

CLARKSON
University

DAA/LANGLEY

IN-CAT. 76

76296

BRIDGMAN CRYSTAL GROWTH

P. 12

February 1987

Prepared by:

Frederick M. Carlson
Clarkson University
Potsdam, New York 13676

(NASA-CR-180958)
(Clarkson Univ.)
A02/MF A01

BRIDGMAN CRYSTAL GROWTH
12 p Avail: NTIS HC
CSCL 20B

N87-27008

Unclas
G3/26 0076296

NASA Grant No. NAG-1-397

Prepared for:

NASA Langley Research Center
Hampton, Virginia 23665

INTRODUCTION

The tasks proposed in our last proposal have been met and additional information generated. The July 1986 Progress Report has been modified and sent to The Journal of Crystal Growth to be published. The article, entitled "The Effect of Gravitational Field Strength on Steady Thermal Convection in Bridgman Stockbarger Crystal Growth," is an extension of the data presented at The Gordon Conference in 1985. These results should be of considerable interest to the crystal growth community.

DISCUSSION OF PROGRESS

The primary focus during this reporting period has been on completing a simulation of thermosolutal convection. The configuration employed was based on some MIT experiments using a Germanium-Silicon charge in a quartz ampoule with an aspect ratio of 8 and a rather large adiabatic zone as given in Fig. 1. Two thermally stable cases were investigated: case A, solutally unstable, and case B, solutally stable. Both use the same equilibrium phase diagram (Fig. 2) and thermophysical properties except the sign of the solutal coefficient of volume expansion is reversed. Initially the ampoule is placed midway in the adiabatic zone and is in a steady state thermal convection mode with a zero pull rate ($V_p = 0$). The gravity level is $9.8(10^{-4}) \text{ m/s}^2$ and an interface temperature ($T_f = 937.4^\circ\text{C}$) corresponding to a zero concentration in the melt presides.

At time equal to zero the ampoule pull rate is increased to $1.39(10^{-5}) \text{ m/s}$ and a uniform melt mass fraction, C , of 0.2 is impressed on the system. Case A will be described first followed by differences between the cases. The interface position as the solidification progresses through the ampoule is shown in Fig. 3. No movement is indicated in the first 200s as the interface temperature adjusts to its new lower equilibrium value. The crystal was not allowed to melt. A more realistic situation would have been a melt back followed by a resolidification. Between 200s and 700s a transient growth phase where interface growth rate, V_f , and pull rate are not the same. The initially planar interface now becomes concave and the curvature continues to change with time. Following this a steady state phase from 700s to 1370s occurs in which pull rate and growth rate are equal. Bulk concentration continually changes during all phases of the process. Finally, the side of the ampoule is lowered to a position within the adiabatic zone, and since the top is insulated, rapid solidification ensues until the entire charge is crystalized at 1810s.

Figure 4 shows the concentration field throughout the charge at 748s. Notice that the interface is not at a constant axial location but varies with radius. In this plot it lies between $z = 4.05$ and 4.15 . Inspection will reveal that the interface is concave. The liquid region immediately in front of the interface indicates a thin layer (approximately 0.5 cm) of rapidly decreasing concentration. This is the concentration "boundary layer". There

is also a radial gradient in the liquid(say at $z = 5.5$) outside this layer due to advection(a single cell, more later) in the bulk. This contrasts with the dual celled solutally stable case B which has a corresponding smaller gradient.

At 1810s the charge is completely solidified. The C distribution in the solid will be examined using Fig. 5 and Fig. 3.

3.5 < z < 3.75, ($0 < t < 450$ s)

Initial transient period, interface adjusting to the step change in bulk concentration. The interface temperature must drop from 937 to 918 °C. $V_f = 0$ until about $t = 200$ s. Then V_f increases from zero to some value greater than V_p and C_s increases. C_s increases because solute cannot "escape" to the bulk but instead is "trapped" in the solid.

3.75 < z < 4.0, ($450 < t < 700$ s)

V_f decreases and then increases. Corresponding to this C_s increases and then decreases. This always happens and others have noticed it [e.g., Smith, Tiller, Rutter, Canadian J. of Physics v33 no. 1 (1955) 723-745, and Bourret, Derby, Brown; J. Crystal Growth 71 (1985) 587-596.].

4.0 < z < 4.9, ($700 < t < 1400$ s)

"Steady state" growth with continuous change in C-bulk. $V_f = V_p = 1.39(10^{-5})$ m/s = slope of curve in Fig. 3. Note the large radial segregation.

4.9 < z < 7.5, ($1400 < t < 1800$ s)

Side of the ampoule now entirely within the adiabatic zone. No energy enters the charge since the top of the ampoule is insulated. V_f exceeds V_p as shown. This increase in V_f dictates an increase in C as previously mentioned, but the overall species concentration demands a general decrease. The characteristic increase in C in the vicinity of the "last to freeze" is not quite as dramatic as it should be because of the rather large computational volumes and the averaging used.

Two curves corresponding to those just presented are given in Figs. 6 and 7 for solutally stable case B. Differences between the two cases will be noted below with the aid of Table 1. Case A is primarily single celled advection with a second, much weaker cell appearing for short time intervals but always fading. The melt velocity increases from the initial thermally driven condition to $3.62(10^{-2})$ cm/s and then decreases. The interface is essentially planar from the ampoule centerline to about $r/R = 0.5$ after which it becomes concave.

In case B, two counterrotating cells are present for most of the process except at the very beginning and end. The melt velocity is maximum at $2.0(10^{-2})$ cm/s at time equal to zero and then steadily decreases to zero. The

upper cell is always stronger than the lower cell but is extinguished at the end of the process before the lower cell. The magnitude of the maximum velocity is always less than case A at corresponding times. The concave interface is usually planar between $r/R = 0.0$ and 0.7 .

Initially: C=0, Thermal Convection

$$\psi_{\max}=1.1(10^{-3})\text{Cm}^3/\text{s}, \quad V_{\max}=2(10^{-2})\text{Cm}/\text{s}$$

Solutally Unstable

t(sec)	0	280	506	748	1078	1392	1441	
$\psi_{\max}(\frac{\text{Cm}^3}{\text{s}})$	1(10 ⁻³)	1(10 ⁻³)	1.74(10 ⁻³)	1.62(10 ⁻³)	1.7(10 ⁻³)	6.1(10 ⁻⁴)	7.4(10 ⁻⁵)	Primary Cell
	x	x	x	-6.9(10 ⁻⁸)	x	-2(10 ⁻⁶)	x	Secondary Cell
$V_{\max}(\frac{\text{Cm}}{\text{s}})$	2(10 ⁻²)	1.96(10 ⁻²)	3.6(10 ⁻²)	3.3(10 ⁻²)	3.6(10 ⁻²)	1.2(10 ⁻²)	1.2(10 ⁻³)	

Solutally Stable

t(sec)	0	288	505	747	1085	1400	1448	
$\psi_{\max}(\frac{\text{Cm}^3}{\text{s}})$	1(10 ⁻³)	9.2(10 ⁻⁴)	7.5(10 ⁻⁴)	5.4(10 ⁻⁴)	3.6(10 ⁻⁴)	7.5(10 ⁻⁶)	x	Primary Cell
	x	-3.5(10 ⁻⁶)	-1.9(10 ⁻⁶)	-6.8(10 ⁻⁶)	-6.5(10 ⁻⁶)	-8.4(10 ⁻⁶)	-2.7(10 ⁻⁷)	Secondary Cell
$V_{\max}(\frac{\text{Cm}}{\text{s}})$	2(10 ⁻²)	1.8(10 ⁻²)	1.5(10 ⁻²)	1.1(10 ⁻²)	7.1(10 ⁻³)	1.6(10 ⁻⁴)	6.0(10 ⁻⁶)	

Table 1

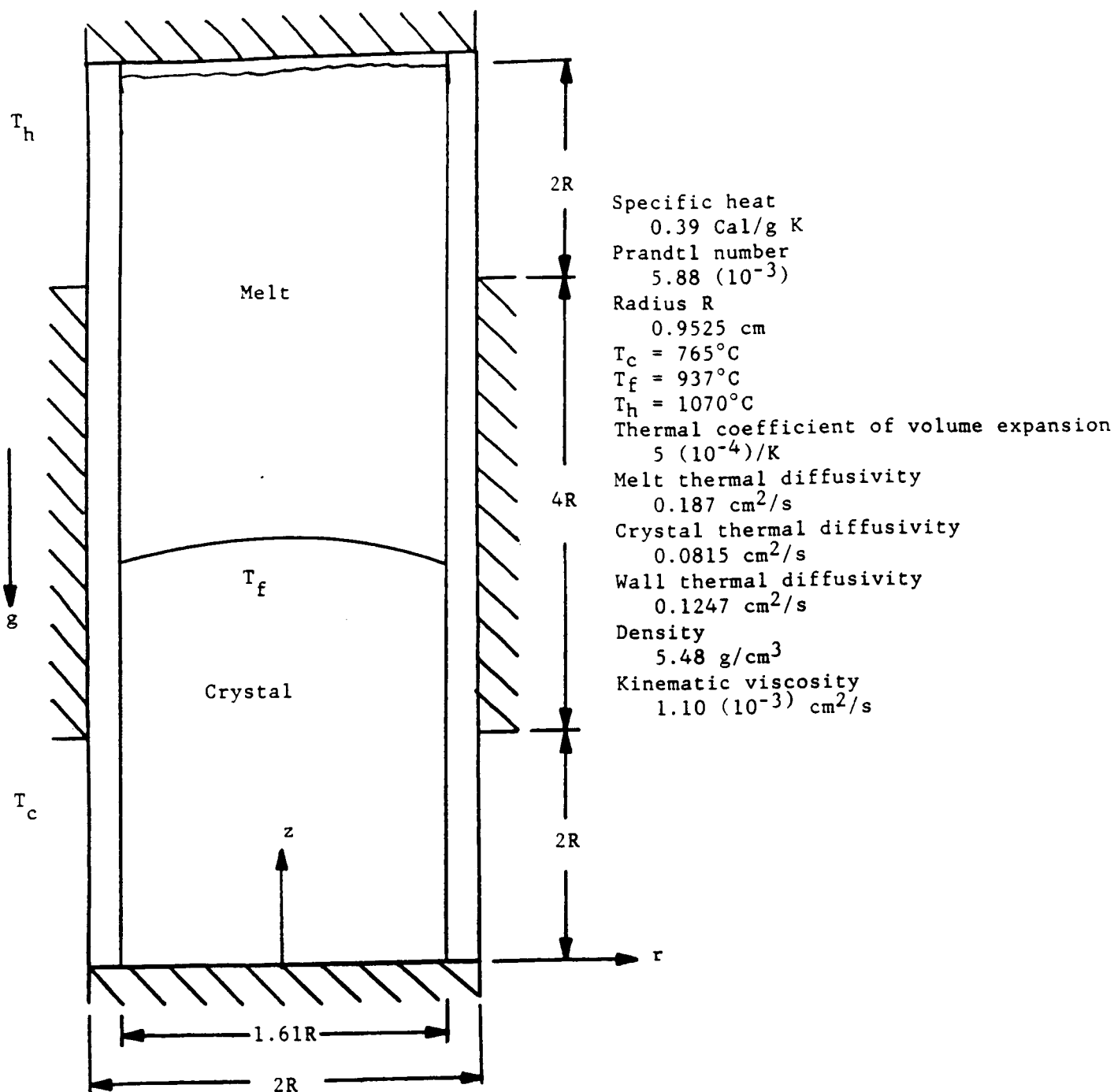


Figure 1. Schematic of Bridgman-Stockbarger System and Thermophysical Properties

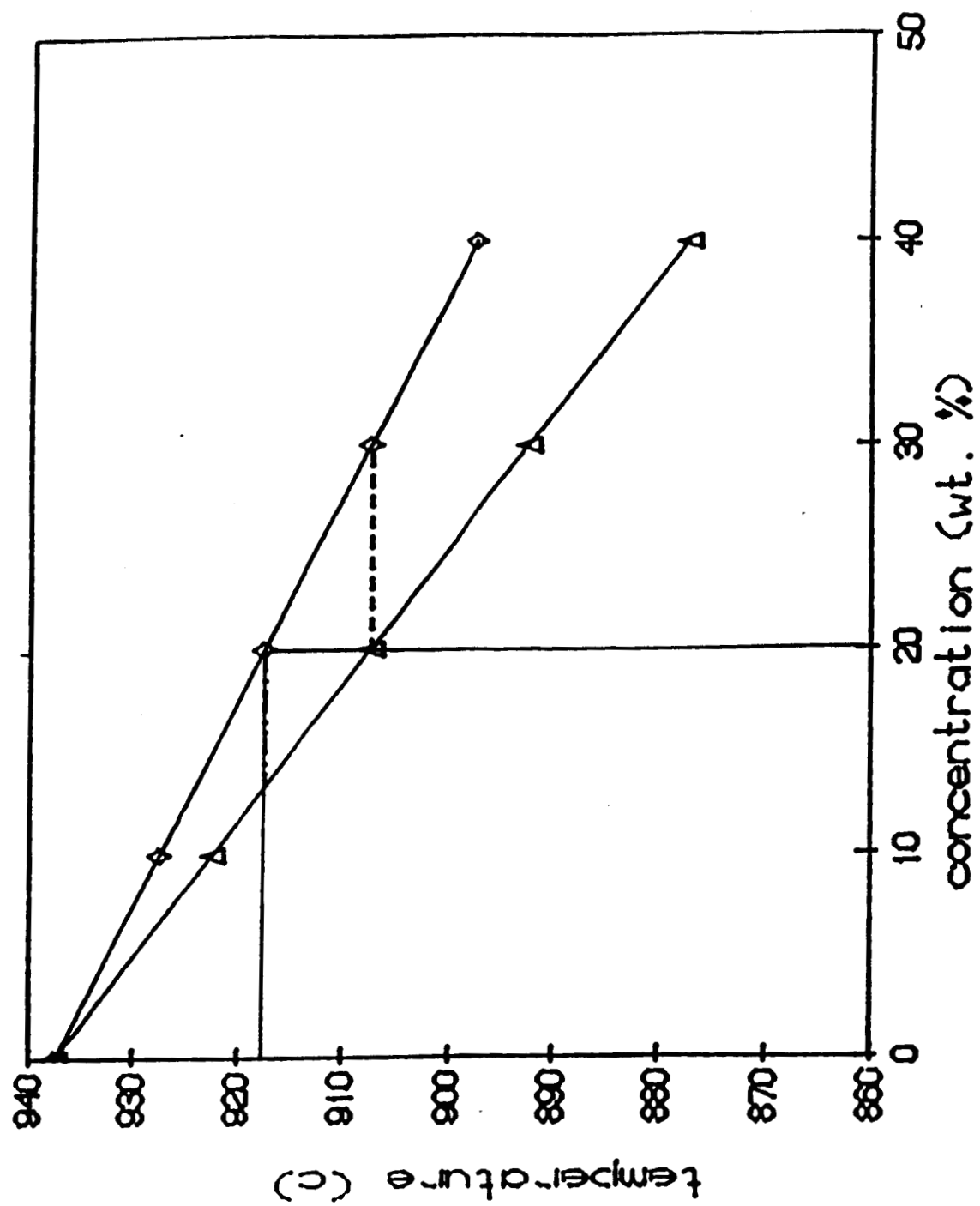


Figure 2. Phase Diagram

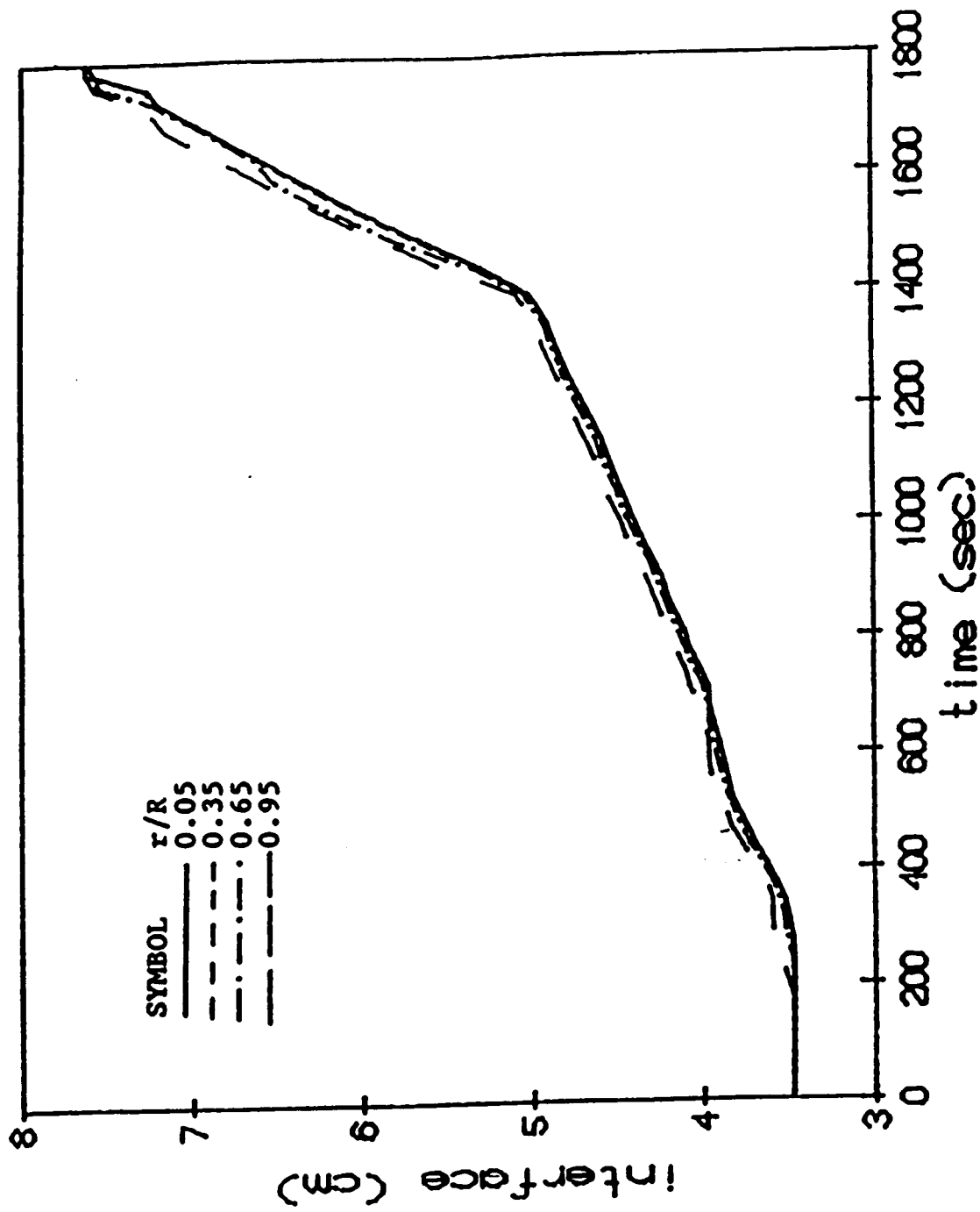


Figure 3. Interface position versus time for thermally stable, solutally unstable convection.

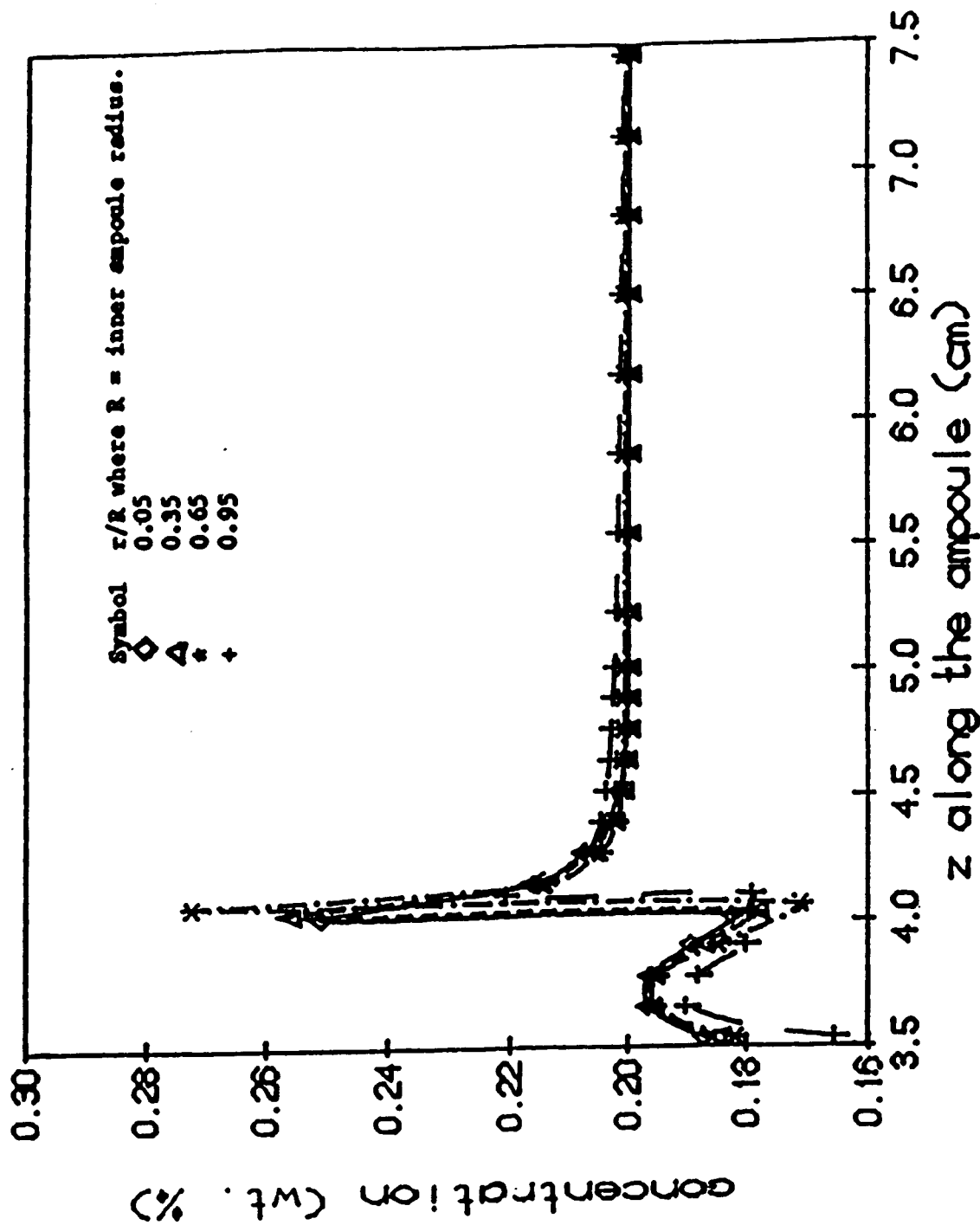


Figure 4. Charge concentration field when partially solidified at 506 seconds.
Thermally stable, solutally unstable.

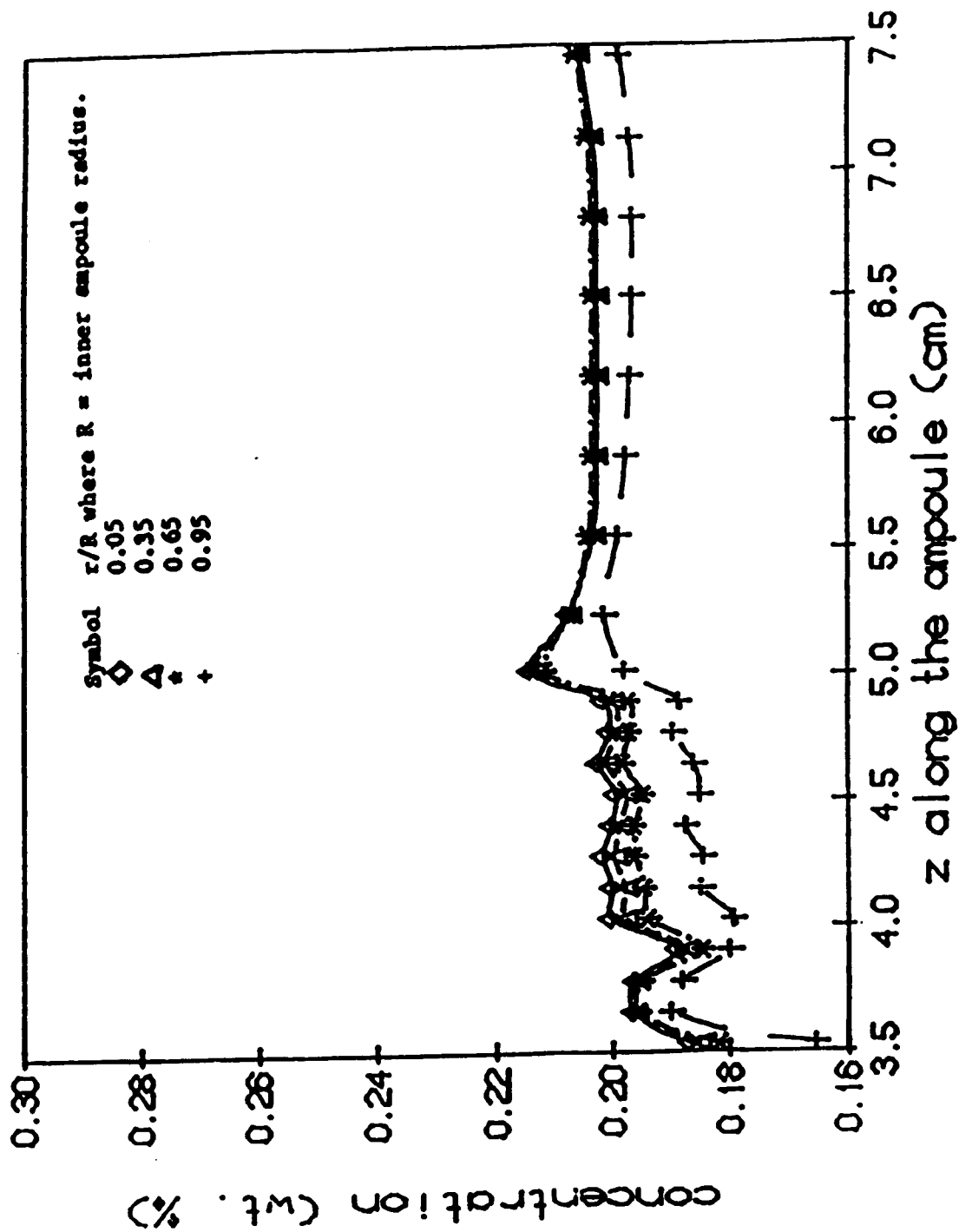


Figure 5. Charge concentration field when completely solidified at 1810 seconds. Thermally stable, solutally unstable.

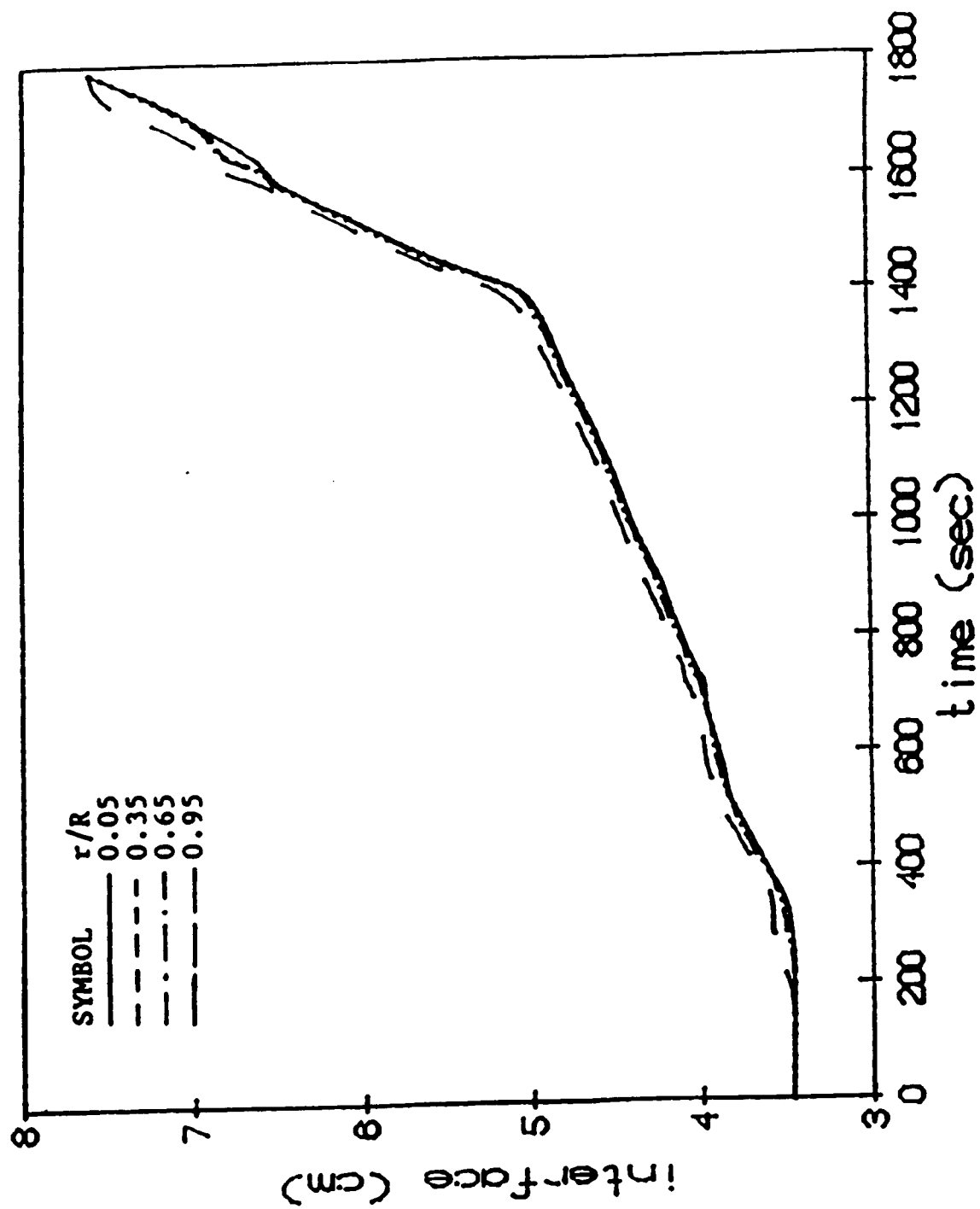


Figure 6. Interface position versus time for thermally stable, solutally stable convection.

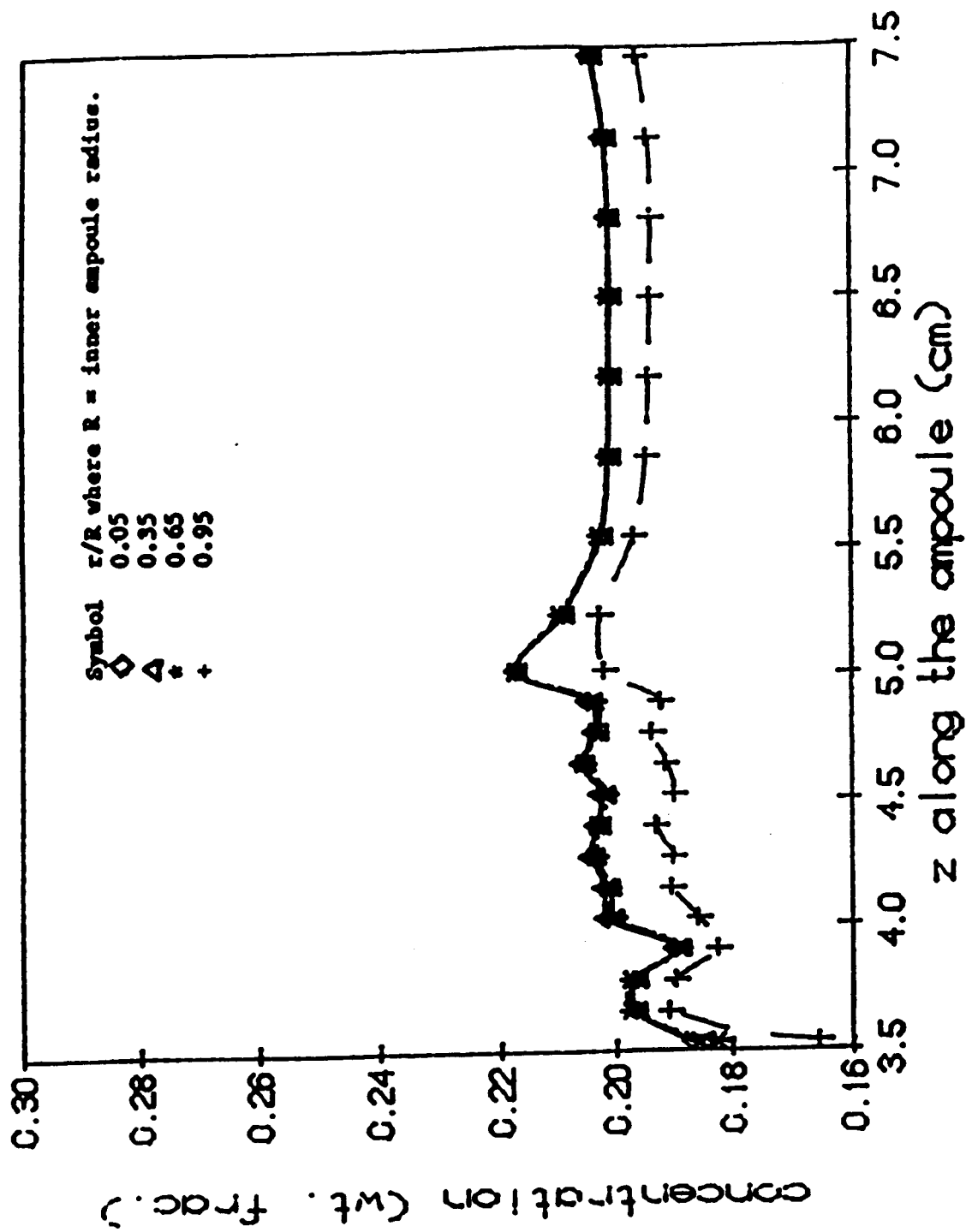


Figure 7. Charge concentration field when completely solidified at 1800 seconds.
Thermally stable, solutally stable.